May 9, 1996

CLOSE PROXIMITY AND LANDING ORBITS AT ASTEROIDS

D.J. Scheeres
Jet Propulsion Laboratory
California Institute of Technology
MS 301-125J
4800 Oak Grove Drive
Pasadena, California 91109-8099
Phone (818) 354-7128
FAX: (818) 393-6388
email: dan.scheeres@zeus.jpl.nasa.gov

Abstract

This paper discusses and describes the dynamics and control of a spacecraft orbiting close to or landing on an asteroid or comet. The paper reports analytical and numerical results which illustrate the challenges facing near asteroid orbiters. Included are a variety of formulae which give order of magnitude calculations of relevant dynamical quantities useful for design and feasibility studies. In particular, we discuss orbit determination and control, orbital dynamics, close proximity operations and landing operations.

Some applications of these results to the NEAR mission to Eros are given, with an eye towards a potential landing phase for that mission.

1 Introduction

Small bodies, such as asteroids and comets, have been of increasing interest lately. This is driven by several factors, including a desire to uncover the primal constituents of the solar system, to further our understanding of dynamical processes in the solar system and to better understand those objects which occasionally impact with the earth and the other planets. Additionally, near-earth asteroids are, in some sense, inexpensive to rendezvous with and thus are prime candidates for lower-cost missions.

In response to such interest, there has been an increase in the number of proposed missions to such bodies. A common feature of many of these proposals is a phase of orbiting close to the body and perhaps a landing phase when in situ measurements can be acquired. Also, of great significance, is the NEAR mission to the asteroid Eros, whose nominal mission contains periods of close proximity operations and whose extended mission may include a landing phase. This paper is meant to address some of the basic questions that must be dealt with in these situations and provide useful and relevant design formulae with which to analyze some of the dynamical concerns that are faced.

First, a discussion on the navigation of close proximity and landing orbits is given. A distinction is made between ground-based and autonomous navigation approaches, realizing that any feasible realization must includeel ments cf oth Following this is a section on the dynamics of close orbiters, concentrati ng on the effects of the 2nd degree arid order field, which dominates the interesting S/C dynamics at the time scales of int erest. The severe shape distortion commonly found at small bodies yields large changes in the orbita elements of a S/C, and leads to limits on what types of orbits arc feasible to fly. Then sections de ling specifically with close proximity and landing operations are given. These sect ions contain relevant design formulae which show the feasibility or non- feasibility of certain approaches. Some specific examples arc applied to the NEAR mission and its options during the follow-on phase

This paper strives fOr generality in its discussion dynamics about small bodies, as there is a large range in the sizes, shapes and properties of these bodies. This becomes evident in the notation used, where the body density ρ and mean radius 7 a left as free variables. Thus, in discussing the gravitational attraction of a small body we must u al with the mass constant $\mu = 4\pi G \rho r_o^3/3$, where μ is the gravitational constant in km^3/s^2, (: 6 672 x 10^{-8} $cm^3/g/s^2$, p is the density measured in g/cm^3 and r_o is the mean radius of the body measured in km. As an example, consider the circular speed of a S/C about a small body, usually expressed as $V_{lc} = \sqrt{\mu/a}$ where a is the semi - major axis and μ is the gravitational parameter. In this paper, this speed is instead expressed as: $V_{lc} = 0.53\sqrt{\rho/\tilde{a}}\, r_o$ m/s, where ρ is the body density measured in g/cc, r_o is the body's mean radius in km and $\tilde{a}$ is the semi-major axis normalized w. it , rc.s])(.et, to the mean radius. The two equations arc equivalent, yet the second form provides the reader with a more immediate, and understandable, result.

This paper only considers the force effects due to the small body's gravity field, ignoring the effect of the solar tide and solar radiation pressure on the orbital evolution. This assumption is justified, as at the close radii assumed herein the effect of these other perturbing forces is small over the time spans of interest ([22]). '1 he discussions here are also relevant for comets, although the outgassing forces which may be found at such bodies are not taken into account, thus the analysis is more relevant for near-dead comets or comets prior to excitation.

2 Navigation and Control Issues

A brief review of the relevant navigation data types operations strategies and control methodologies is given. The emphasis is describing the different approaches and indicating the limiting factors for achievable accuracy with on-board (potentially autonomous) observations.

2.1 Ground-Based Orbit Determination

Ground- based orbit determination for a small body mission will generally consist of a combination of radiometric, optical and (potentially) altimetry data. See papers [16] and [20] for a description of the necessary approaches and potential accuracy of this approach. Especially note paper [16] which gives a description of how the Near Earth Asteroid Rendezvous (NEAR) mission will be navigated from the ground during the orbital phase

The main characteristic of' ground based orbit determination is the high accuracy which is obtainable, leading to precise models of the small body, its force environment and the S/C orbit about it . For the immediate future ground-based orbit determination will play an important role in defining the body models which will be used in autonomous navigation systems.

The weakness of ground-based orbit determination is the long turn around times, limited at best by the round-trip light time. This delay makes many types of close-proximity and landing orbits uncontrollable, in that, the reaction time is not sufficiently swift to correct errors and to control the S/C to a nominal trajectory. '1'0 navigate, small body mission from the ground alone will place hard constraints on the mission design and on the achievable science return.

If an efficient ground system is (it:.M,rI(ew hic can turn radiometric and optical measurements into orbit corrections on a short time scale, these ground systems may st ill be feasible to use for some classes of close proximity orbits. There are however, a great number of constraints that would come with such a system, not the least of which is the need to dedicate antenna time over long periods to enable the ground system to respond appropriately during the period of close operations.

In closing, it should also be noted that whenever communication takes place between the S/C and the ground, data suitable for high-accuracy orbit determination becomes available at essentially no extra cost. Thus, once a body is encountered and the science data is sent to Earth and the specific instructions are sent to the S/C there will be data suitable for high precision orbit and model determination.

2.2 On-Board (Autonomous) Orbit Determination

In contrast with the ground based solution are on-board orbit determinations. The types of measurements usually considered for autonomous systems are optical and altimetry measurements. The optical measurements will either image the limb or surface landmarks of the body and correlate these images with an existing model of the body to generate the residuals. These measurements can be combined to yield S/C position fixes. Estimates of the S/C speed must rely on position measurements tied together over time using known models of the body. For instance, in Reference [1] it is noted that the velocity determination becomes much better when the S/C is tracked over several revolutions, as then the filter can use the total mass of the body (which will be well known in general) to aid in fitting the positions to the true orbit.

Methods to perform each of these types of measurements and reductions have been developed, in the case of limb sensing an autonomous scheme has been developed and tested and proven to work well under fairly benign orbital conditions ([1]). Similar techniques may be possible for landmark tracking ([8]). Two such optical sightings of the body surface are sufficient to determine the instantaneous position of the S/C with respect to the body, assuming that a model of the body exists. The ability to limb track becomes limited as the S/C altitude decreases, as the process of correlating the imaged limb to the stored model becomes more difficult when the body limb lies near the horizon. In this regime it is better to image landmarks on the body's surface and correlate them with the internal model to determine which landmarks the S/C is looking at. Having determined this, an instantaneous position measurement can be constructed given two such sightings. The landmark approach requires a more detailed map of the surface, yet may only be necessary for those portions of the surface over which the S/C will hover closely. If the S/C comes very close to the small body surface, landmark tracking becomes less practical as well. First, to continue to reliably track landmarks will require that a high resolution model be aboard the S/C. Second, the altitude determination will be limited by the model error and may not allow for a closed-loop soft landing.

In other situations it is desirable to incorporate altimetry into the navigation system. Altimetry measurements alone do not suffice to determine position, unless they are used to perform limb-scans or processed over long time spans. To compute a complete solution from altimetry alone requires that the data be accumulated and stored over fairly long time spans and processed against the existing models of the body, an approach more suited to ground operations. Altimetry data used in conjunction with landmark observations however, is a strong data type and would be essential for soft-landing operations. It's best feature is that it's altitude determination of the S/C is independent of the modeling error.

Limb tracking is most feasible when a few radii from the body, landmark tracking is most feasible when closer to the body and altimetry becomes important when considering orbits close to or landing on the surface. Essential to all autonomous navigation measurements are accurate S/C attitude estimates and precise control.

Of interest is the accuracy of these different orbit determinations. The relevant quantities in terms of accuracy are the angular fix of the S/C in the body-fixed space (i.e. the error in the latitude and longitude of the S/C), the S/C radius with respect to the body center of mass and the S/C altitude above the body surface. For all combinations (limb, landmark and landmark+altitude) the determination of the radial and angular position of the S/C is proportional to σ_{r_o} and σ_{r_o}/r_o respectively, where σ_{r_o} is the overall error in the body model (in length units) and r_o is the mean radius of the body. The proportionality factor for each position fix ranges from 1 to $\sqrt{2}$, depending on the combination. The determination of altitude is usually only performed using landmark tracking alone or in combination with altimetry. For landmark tracking alone, the altitude determination from one position fix is approximately $\sqrt{3}/2\sigma$, „ while for landmark plus altimetetry the accuracy is the accuracy of the altimeter measurement which may be on the order of centimeters or meters. For all these results, it is assumed that the optical and altimetry data is obtained at "optimal" viewing conditions. For land mark tracking this means that 1 he two landmarks lie 45 deg rees off nadir in opposite directions, for landmark plus altimetry this means that the landmark lies at nadir.

2.3 Constructing the Small Body Model

The observat ions from the previous section on the accuracies of orbit determination bear on the ability of a S/C to aut on om ously estimate a model of the small body about which it is orbiting. As the position and orbit determinations are all at lea I partly limited by the uncertainty of the body model, it becomes more difficult to estimate a mod of the body as this must be done in tandem with the orbit determination.

'J>o reliably perform this determination wo ld require severa I pre-requisites: a stable and predictable orbit to perform the determination from, a reasonable span of time to allow for "$\sqrt{N}$" effects to increase the accuracy of the model, high resolution instruments to allow for accurate models to be constructed from orbits far enough from 1111 th body to minimize gravitational perturbations. Note, altimetry measurements would be useful for such a determination as they would provide a metric measurement (unlike the exclusively angular measurements of the optical system) and could be used to define the overall size and volume of th body which would allow for the proper scale to be applied to all the optical measurements.

Given that such an estimation could I performed autonomously, it would always lag behind the model accuracy possible using the ground system. This is mainly due to the extreme accuracy of the Doppler measurements and its ability to determine the total mass and gravitational field to high accuracy. Given this base information, the model can be estimated from the optical and altimetry data using their full accuracy, instead of watering down these measurements by determining the orbit simultaneously.

One final comparison, for ground based model determination it is possible to estimate the necessary model resolution from further away than for an 011. board determination. On-board determinations require more of a "spiral in' mode when the lower orbit determination accuracy requires the S/(; to estimate the small body model from a closer orbit, which in turn induces its own errors etc...

2.4 Methods of Control

Given an orbit determination and prediction capability, the control of the S/C orbit must be considered. The orbit control strateg ies can be divided into three general areas, analytic predictors, numerical targeting and closed-loop control The divisions are somewhat arbitrary, but are useful for categorizing the different control possibilities.

2.4,1 Analytic Prediction

This app roach uses approximate solutions 1, to orbit dynamics problem to predict the future evolution of the orbit. '1'hen, given that I h o it should pass through some position or satisfy some criterion at a future time, the analytic (or semi analy tic) theory is used to determine what the current orbit should be for the future event to be sat isfied. This approach is most often used for the design of missions on the ground although it could have applicability for some autonomous missions, if precision control of the S/C orbit is not a premium.

This approach fails when orbiting in regimes of motion where the perturbations acting on the S/C are large or the motion chaotic '1 hen, such regular theories will usually not apply. In terms of ground based design, analytic theories may still be constructed for these reg imes and used for high-level design, however they may not be precise enough for an autonomous control scheme due to the inherent non-linearities of the dynamics in these cases.

This approach works best when the dynamics of the S/C orbit can be modeled using averaging techniques. Then, this is useful for designing a mission and computing the proper controls to execute. Regimes where this applies are for retrograde orbiters around uniformly rotating small bodies and for S/C orbits far from the small body, where tidal and solar radiation pressure forces become important. The greatest advantage of this approach is that it uses analytic solutions which are understood and bounded a priori, and does not rely on solutions which may have unpredicted behavior.

2.4.2 Numerical Targeting

In regimes where analytic approaches no longer match with reality it is necessary to use numerical approaches to define and compute quantities of interest. This is always the case with ground based missions, where the S/C trajectory is usually targeted to a location in space at a fixed or variable time. The usual example of this is targeting to the "B-plane" of a body, either fixing the time of closest approach or letting it vary. Numerical targeting is necessary as all the important force perturbations can then be included and modeled appropriately.

This approach can also be used for more esoteric examples and applications, such as the computation of periodic orbits close to the small body. Such orbits exist about small bodies ([18], [19], [21]) and cannot be expressed in analytical form, yet procedures can be developed to compute them as a function of initial state only. This approach can also be generalized to less constraining situations, and can be used to compute circular orbits about small bodies. One can attempt to predict the necessary initial conditions for a circular orbit based on averaging theory or can use a purely numerical approach which fits the orbit to a circular orbit in a least-squares sense. Reference [19] analyses this situation and some other applications in greater detail.

The key for effective numerical targeting is to define the target locations, events or limits in terms of unambiguous geometries, and then develop numerical procedures to satisfy these conditions. Often, this may involve optimization techniques in conjunction with more traditional targeting techniques. Such approaches may not be feasible for autonomous scenarios. Only if the problem can be bounded a priori and the range of expected solutions shown to be well behaved and the targeting schemes uniformly convergent should it be trusted to an autonomous computation. In many instances, such numerical techniques have to be "baby-sat" as the problem being solved is a non-linear problem for which multiple solutions may exist.

2.4.3 Closed-Loop Flight Path Control

The analogue to numerical targeting for autonomous missions is closed loop flight path control. In this situation the S/C explicitly controls itself to a specific flight path (which may either be computed on-board or on the ground). In reality, all ground based control operations also perform a closed-loop flight path control, except the systems are designed so that the orbit is stable with a control delay of days or weeks. This is usually done by performing very accurate orbit determination and targeting of the nominal S/C orbit. Then the frequency of corrections can be decreased appreciably. For intensive operations near the surface of a small body this type of control delay may not be acceptable, and may yield an orbit that is unstable. At best, the ground based control time delay can be reduced to the order of hours which is still not sufficient for close proximity or landing operations. Also, the data types usually used for ground based control do not yield "instantaneous" position fixes, which are useful for closing the S/C control loop.

In these situations it becomes necessary for the appropriate measurements to be made on-board and used to alter the control law to fly back to some pre-programmed nominal flight path. At smaller bodies (or less massive bodies) the S/C can "remove" the body's gravitational field in some instances by using models to generate thrust laws. This will, in general, require autonomous orbit determination to implement and is probably the most attractive mechanism by which to come close to the surface of a small body for a sustained period of time. To do this requires a variable thrust engine. If not available, this approach is made much more difficult, and perhaps is not realistically computable.

If only a fixed thrust system is available then all control maneuvers must be implemented as finite-time maneuvers. For deep space missions this entails no real complications, however for operations close to a body this will complicate the execution of maneuvers and the control algorithm, and should be studied further.

3 Dynamics of Close Orbiters

Of great importance in controlling and designing close proximity and landing orbits at a small body is an understanding of the dynamics of orbits close to these bodies. This section gives a brief review of this problem, cites appropriate texts for previous work done in this area and gives a sketch of the current state of understanding in this area.

3.1 Problem Definition and Derivations

The equations of motion for a S/C close to a small body (usually within 10 radii for the effect of the solar tide and radiation pressure to be ignored, see [19] and [22]) are stated in the small-body fixed frame as:

$$\ddot{\mathbf{r}} + 2\Omega \times \dot{\mathbf{r}} + \Omega \times (\Omega \times \mathbf{r}) + \dot{\Omega} \times \mathbf{r} = U_{\mathbf{r}} \tag{1}$$

where $\mathbf{r}$ is the position vector of the S/C in the body-fixed frame, Ω is the rotational velocity of the small body in the body-fixed frame, $U_{\mathbf{r}}$ is the gravitational acceleration and $(\dot{\ })$ denotes the time derivative with respect to the body-fixed coordinate frame.

The gravitational potential U of the small body is usually computed with spherical harmonics when outside the circumscribing sphere about the body or using a collection of N tetrahedra (essentially modeling the body as some arbitrary polyhedron) when close to the surface (note that there is a closed form formula for the gravitational potential of a tetrahedra, see [24]). Approximating the body as a general polyhedron when close to the surface works appreciably better than filling up the shape model with a collection of point masses ([25]).

In terms of the rotational dynamics of the small body, there are two broad classes which apply. If the body is a principal axis rotator (PA), or if it is a non principal axis rotator (NPA). If the body is in PA rotation, then the rotational velocity Ω is constant in the body-fixed frame and the equations of motion have a Jacobi integral ([21][19], [18]). If the body is in NPA rotation, then for the time spans of interest it is acceptable to model the rotational dynamics as occurring in torque free space. Then, the angular velocity will follow the well known motion of a rigid body in free space and can be expressed in terms of elliptic functions ([14]). In this case Ω is no longer constant in the body-fixed space and, consequently, the Jacobi integral is no longer conserved.

For purposes of practical design and understanding of S/C dynamics over fairly short time spans (on the order of weeks or months) it is usually sufficient to only consider the 2nd degree and order gravity field of the body. Depending on the rotational state of the small body, different orbital theories and approximations can be applied. In the following sections we pass along some recent results discovered concerning the dynamics of a S/C about a small body.

3.2 Principal-Axis Rotators

The most important effect on S/C orbits at principal-axis (PA) rotators concerns the interaction, or lack of interaction, between the rotation rate of the body and the rotation rate of the orbit. The primary effect, from an analysis point of view, is due to the 2nd order gravity field, which consists of the two gravity coefficients C_{20} and C_{22}. The gravity potential of this degree is:

$$U_2 = \frac{\mu}{r^3}\left[\frac{r_o^2 C_{20}}{2}\left(3\sin^2\alpha - 1\right) + 3r_o^2 C_{22}\left(1 - \sin^2\alpha\right)\cos(2\lambda)\right] \tag{2}$$

where μ is the gravitational parameter of the body, α is the declination of the S/C in the body-fixed frame and λ is the longitude of the S/C in the body-fixed frame.

3.2.1 C_{20} Gravity

Averaging theory works well to describe the main perturbations that C_{20} gives to a S/C orbit. Averaging the U_{20} potential over the mean anomaly yields the perturbation function:

$$R_{20} = \frac{\mu r_o^2 C_{20}}{2a^3(1-e^2)^{3/2}}\left(\frac{3}{2}\sin^2 i - 1\right) \tag{3}$$

Substituting this in the Lagrange equations of motion shows that the semi-major axis, eccentricity and inclination suffer no secular perturbations due to this term. The remaining orbital elements of argument of the ascending node, argument of periapsis and the mean epoch all have secular terms:

$$\dot{\Omega} = A_{20}\cos i \tag{4}$$

$$\dot{\omega} = A_{20}\left(\frac{5}{2}\sin^2 i - 2\right) \tag{5}$$

$$\dot{M}_o = n\left[1 - A_{20}\sqrt{1-e^2}\left(\frac{3}{2}\sin^2 i - 1\right)\right] \tag{6}$$

where

$$A_{20} = \frac{3 n r_o^2 C_{20}}{2a^2(1-e^2)^2} \tag{7}$$

$$\sim 16\cdots\frac{C_{20}\sqrt{\rho}}{\tilde{a}^{7/2}(1-e^2)^2}\ \text{degrees/hour} \tag{8}$$

Converting these expressions to change in Ω, ω and M_o per orbit yields a coefficient:

$$2\pi A_{20}/n \sim 540\frac{C_{20}}{\tilde{a}^2(1-e^2)^2}\ \text{degrees/orbit} \tag{9}$$

One can show that, in general, $C_{20} < 0.05$ thus this constant is less than $27/\tilde{a}^2$ degrees/orbit for a circular orbit. Due to this strong orbit precession, it is impractical for a low orbit about a small body to maintain an inertially fixed orbit except for inclinations of $i = 0, 90, 180$ degrees. It also implies that the orbit period can also become significantly modified.

3.2.2 C_{22} Gravity

The potential term for C_{22} explicitly contains time in the expression for the S/C longitude. This complicates the procedure of determining the secular effects of this gravity term. Most classical studies of this problem have only looked at the application to Earth, for which the effect is small, and have not considered what the secular effects of this gravity term are in general. For small bodies, where this term can become quite large, the effects become dynamically significant and affect the orbit semi-major axis, eccentricity and inclination in a potentially major way.

Instead of dealing with the semi-major axis and eccentricity directly, it is more useful to consider the orbit energy $C_2 = -\mu/(2a)$ and the angular momentum $h = \sqrt{\mu a(1-e^2)}$. It has been established that interaction of the S/C orbit with the C_{22} coefficient can cause a particle's energy to go from a negative (bound) value to a positive (hyperbolic) value and vice-versa ([18], [19]). Working with the orbit energy and angular momentum allow for the orbit to change from hyperbolic to elliptic or vice-versa without singularity.

There are two approaches for deriving the dynamical effect of C_{22} on these variables, by deriving the differential equation directly or by averaging the potential prior to defining the differential equations. We are interested in determining the change in these variables over **one** passage through periapsis, either from apoapsis to apoapsis or from $-\infty$ to $+\infty$ for a hyperbolic or parabolic orbit. The change in energy as computed from the averaged potential is different from the change in energy as computed directly from the relevant differential equation. We will show these differences and discuss them briefly.

Given an averaged potential, the differential equation for the change in orbital energy is:

$$\dot{C}_2 = \frac{\partial R_{22}}{\partial M_o} \tag{10}$$

where the averaged potential is:

$$\begin{aligned} R_{22} = & \frac{6n^2}{\pi(1-e)\sqrt{1-e^2}} r_o^2 C_{22} \Big[\cos^4 i/2 \cos 2(\nu + \Omega + kM_o) I_2^1(e,k) \\ & + \sin^4 i/2 \cos 2(\nu - \Omega - kM_o) I_{-2}^1(e,k) + \frac{1}{2}\sin^2 i \cos 2(\Omega + kM_o) I_0^1(e,k)\Big] \end{aligned} \tag{11}$$

Starting from first principles, however, the exact differential equation is derived to be:

$$\dot{C}_2 = \frac{dU_{22}}{dt} = \nabla U_{22} \cdot \mathbf{v}_I \tag{12}$$

where U_{22} is the gravity potential of the C_{22} gravity coefficient and the time derivative is taken with respect to the inertial reference frame. To reduce these two equations to a form suitable for comparison, integrate both over one orbit from apoapsis to apoapsis (or from $-\infty$ to $+\infty$ for a parabolic or hyperbolic orbit). For the averaged differential equation, this just involves multiplying by $2\pi/n$. For the exact differential equation this involves an integration equivalent to the averaging process, although yielding different results for the e term. The result is a change in **orbit** energy **over** one **orbit**:

$$\begin{aligned} \Delta C_2 = & -12 r_o^2 C_{22} \frac{\mu}{q^3} \left(\frac{1-e}{1+e}\right)^{3/2} k \Big[\cos^4 i/2 \sin 2(\nu + \Omega + kM_o) I_2^1 \\ & - \sin^4 i/2 \sin 2(\nu - \Omega - kM_o) I_{-2}^1 + \frac{1}{2}\sin^2 i \sin 2(\Omega + kM_o) I_0^1\Big] \end{aligned} \tag{13}$$

or

$$\begin{aligned} \Delta C_2 = & -12 r_o^2 C_{22} \frac{\mu}{q^3} \Big[\cos^4 i/2 \sin 2(\nu + \Omega + kM_o)\left\{I_2^3 + \frac{3e}{4(1+e)}(I_3^2 - I_1^2)\right\} \\ & + \sin^4 i/2 \sin 2(\nu - \Omega - kM_o)\left\{I_{-2}^3 + \frac{3e}{4(1+e)}(I_{-3}^2 - I_{-1}^2)\right\} \\ & + \frac{3e}{8(1+e)} \sin^2 i \sin 2(\Omega + kM_o)\left\{I_1^2 - I_{-1}^2\right\}\Big] \end{aligned} \tag{14}$$

Pertaining to the averaged and exact equations respectively. The functions $I_m^n(e,k)$ are defined as:

$$I_m^n(e,k) = \int_0^{f_\infty} \left(\frac{1+e\cos f}{1+e}\right)^n \cos(mf - 2kM)\, df \tag{15}$$

where $\theta_\infty = \pi$ if $e \le 1$, and $\theta_\infty = \cos^{-1}(-1/e)$ if $e > 1$, f is the true anomaly of the orbit (defined for elliptic, parabolic and hyperbolic orbits), M is the mean anomaly of the orbit (which is a function of true anomaly for either an elliptic, parabolic or hyperbolic orbit) and $k = \omega/n$, where ω **is tile** rotation rate of the small body, and n is the mean motion of the S/C orbit, or its generalization for hyperbolic orbits. The integrals I_m^n cannot be evaluated in closed form in general, as they contain mixed terms relating the true anomaly and the mean anomaly. They can, however, be evaluated numeric ally and the author has wı it ten cod wh performs thes e evaluations for elliptic, parabolic or hyperbolic orbits.

Clearly, the number of evaluations o the functions I^n_m needed for the averaged case are less thau the exact case. For eccentricities greater han ~ 0.9 the two results agree very well, and the averag ed result cau be used in general t r , centricities less than this the averaged result begin to diverge from the exact results and should not t used.

The equations of change for the other elements of interest (i and h) over one periapsis passage arc:

$$
\begin{aligned}
\Delta i &= 12 r_o^2 C_{22} \frac{\sin i}{q^2(1+e)} \left[\cos^2 i/2 \sin 2(\nu + \Omega + kM_o) I^1_2 \right. \\
&\quad \left. - \sin^2 i/2 \sin 2(\nu - \Omega - kM_o) I^1_{-2} + \sin 2(\Omega + kM_o) I^1_0 \right] && (16) \\
\Delta h &= -12 r_o^2 C_{22} \sqrt{\frac{\mu}{q^3(1+e)}} \\
&\quad \left[\cos^4 i/2 \sin 2(\nu + \Omega + kM_o) I^1_2 + \sin^4 i/2 \sin 2(\nu - \Omega - kM_o) I^1_{-2}\right] && (17) \\
& && (18)
\end{aligned}
$$

The averaged potential results for these elements do not suffer the same problems as for the C_2 term. A c.artful derivation of all these equation show that they are valid for both elliptic (e < 1), parabolic (e = 1) and hyperbolic ($e > 1$) orbits Also useful are linearized expressions for the cha nge in orbit periapsis and eccentricity:

$$\Delta q = (h\Delta h - q^2 \Delta C_2) / (\mu e) \tag{19}$$

$$\Delta e = (h\Delta C_2 + 2C_2 \Delta h) h / (\mu^2 e) \tag{20}$$

It is important to notes that $|I^1_m| \gg |I^1_{-m}|$ for $m >$ **1** general, as it implies that when $i > \pi/2$ that the resulting cha nge in , periapsis for one passage begins to decrease, and that for $i = \pi$, the net change is in fact sm , 1 Indeed, it is when the inclina tion of the orbit is much larger than $\pi/2$, then the dynamics of the orbit can be well approximated by those of au orbiter about an oblate pla net. This also shows that the s/c may be safely flown close **to** the ends of **the** body, if flown in a retrograde orbit.

The following plots give a few applications of these expressions. Plot XX shows, for au inclination of O, the capture and ejection radius of **a** S/C about a small body. Plot 1 shows contours of constant change in apoapsis radius as a function **of** periapsis radius and eccentricity, this plot was generated for a body with $\sqrt{\rho}T = 3.2 (g/cm^3)^{1/2}$ hours, and with a shape with ratios 1 : 0.5 : 0.5.

One final note to make, the change in orbit size and shape can be completely normalized in terms of the body's size. That is, the change in shape and size is only **a** function **of the orbit** shape (eccentr icity) and relative size (periapsis radius expressed in terms of body radii). The body dependent terms which enter the expressions are the non-dimensional gravity coefficient C_{22} and k, where $k \propto 1/\sqrt{\rho}T^2$ aud ρ is the body density and T is the body's rotation period. This allows for general statements to be made about the dynamics of small body orbiters independent of the overall size of the body in question.

3.3 Non-Principal-Axis Rotators

The situation for non-principal axis rotators (NPA's) is considerably different. Bodies with an NPA rotation state arc considerably more rare than their PA counterparts, yet they do exist. Usually, such bodies are comets, although there are a number of confirmed cases of asteroids which arc in an NPA **rotation state** ([9], [15]) **A** common characteristic of all of the NPA asteroids is that their overall angular moment um is quite small, leading to long relaxation times. If this were not the case these bodies would have relaxed into principal axis rotation about their largest moment of inertia within a relatively short time span, as this is the stable ro tational mode for such bodies.

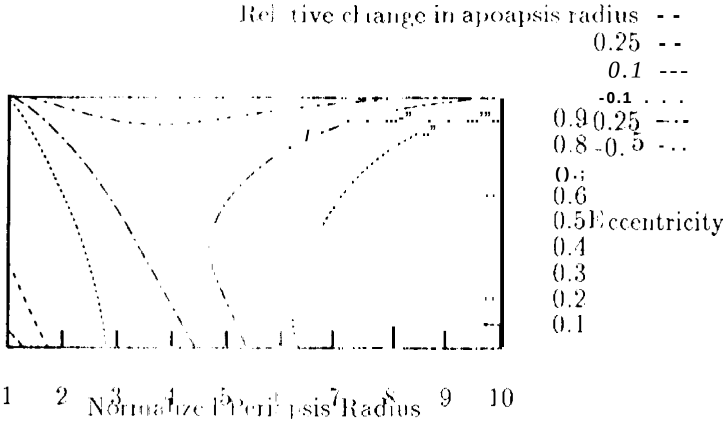

Figure 1: Relative change in apoapsis for one orbit, as a function of normalized periapsis and eccentricity for a 0 inclination orbit with periapsis located 45 degrees ccw from the long end of the body

Since $|\Omega| \ll 1$ in general the transient changes due to the C_{22} term may be ignored, at first order. This is seen in the averaged ΔC result where we note that the change in energy is proportional to the angular velocity of the body rotation rate, a relationship which also holds true for the exact results. Thus, the major dynamical effects are due to the C_{20} coefficient. For longer integration time spans it may be necessary to include higher order terms which yield instabilities (such as C_{30}).

The perturbing gravity potential is then

$$U_{20} = \frac{\mu}{2r^3} r_o^2 C_{20} [3(\mathbf{P}_z \cdot \mathbf{r}_s)^2 - 1] \tag{21}$$

Where $\mathbf{P}_z = [\cos\delta\cos\alpha, \cos\delta\sin\alpha, \sin\delta]$ and is the vector describing the orientation of the symmetry axis of the body in inertial space, where δ is the declination and α the right ascension of the pole and $\mathbf{r}_s$ is the unit vector defining the position of the S/C in inertial space. For NPA bodies, the "pole" of the body may no longer be measured from the maximum moment of inertia, but may also be measured from the minimum moment of inertia, depending on the specific rotation state the body is in. In general, the declination δ and right ascension α are functions of time and can be expressed explicitly in terms of elliptic functions [14]). In general the declination δ will librate about some average value and the right ascension will have a secular increase with time. The particulars of their evolution depends on the body in question, again Averaging this potential over one orbit yields:

$$R_{20} = \frac{n^2}{4(1-e^2)^{3/2}} r_o^2 C_{20} \left[1 - 3(\mathbf{P}_z \cdot \mathbf{r}_h)^2\right] \tag{22}$$

where $\mathbf{r}_h = [\sin\Omega\sin i, -\cos\Omega\sin i, \cos i]$ is the unit vector along the S/C orbits' osculating angular momentum vector. Note that this potential is time varying. The semi-major axis and eccentricity have no secular terms with this perturbing potential. The remaining orbital elements have secular motions described by:

$$\dot{\Omega} = -\frac{na}{\mu\sqrt{1-e^2}} \csc i \frac{\partial R_{20}}{\partial i} \tag{23}$$

$$\dot{i} = -\frac{na}{\mu\sqrt{1-e^2}} \csc i \frac{\partial R_{20}}{\partial \Omega} \tag{24}$$

$$\dot{M}_o = -\frac{2}{na}\frac{\partial R_{20}}{\partial a} - \frac{1-e^2}{na^2 e}\frac{\partial R_{20}}{\partial e} \tag{25}$$

$$\dot{\omega} = \frac{\sqrt{1-e^2}}{na^2 e}\frac{\partial R_{20}}{\partial e} - \frac{\cot i}{na^2\sqrt{1-e^2}}\frac{\partial R_{20}}{\partial i} \tag{26}$$

The **orbital** elements of most interest are the inclination and argument of the ascending node, as this pair form a closed set and their evolution drives the evolution of the other elements.

The motion of this system has a few interesting characteristics. First, the inclination in inertia] space has large, quasi-periodic variation due to the motion of the asteroid in inertial space. In some cases the inclination can cross from direct to a retrograde orbit, or viw-versa. For longer-term integrations, this problem is tied and the effect of the C_{30} term of the gravity field becomes important. The effect of this term is to give the eccentricity a long-term drift. At this level, the theory must combine the inclination, argument of ascending node, argument of periapsis and eccentricity. The relevant analysis is yet to be performed.

A case in point is the asteroid Toutatis, for which an accurate shape model and rotational state exists ([{)]). This asteroid is in non principal axis rotation about its minimum moment of inertia, it's nutation angle is approximately 50 and has a variation of less than one degree. The precessional period in inertial space is approximately 7.54 **days**, Its 2nd order gravity field (with respect to its minimum moment of inertia axis) .

$$r_o^2 C_{20} \quad 0.77705 \text{ km}^2 \tag{27}$$

$$r_o^2 C_{22} \quad 0.0163 \text{ km}^2 \tag{28}$$

Note that the C_{20} term is positive, as expected for a prolate spheroid, and that the C_{22} term is rather small. Following are some plots of the evolution of the inclination and argument of the ascending node, note the quasi- periodic variations in the inclination, which allow the orbit **to** switch between **direct** and retrograde orbits over **1** ime.

3.4 Definition and Computation of Stability Measures

The above, more analytical, theories are useful when considering individual spacecraft orbits or designing specific trajectories. It is also necessary to understand the less tangible **issues** of spacecraft dynamics, **suet] as** when **the S/(; is** in a chaotic zone or when it is in a region **of** bounded motion. Should the orbit lie in, or close to a chaotic region **of** phase space, then the predicted motion of the S/C will be uncertain and the final outcome of a planned orbit in question. When flying close to small bodies, this is a pertinent question For example observe the results of a Monte-Carlo simulation which tracked the final evolution of a few hundred particles drawn about an initial trajectory with a position uncertainty of 5 meters and , v,l , its uncertainty **of** 0.1 mm/sec. Note **that** this small difference in initial conditions leads to drastically different eccentricities and semi-major axes after only ten **days (which** corresponds to approximately one orbit in the nominal orbit). Clearly, the perturbations acting on the orbit are strong enough to be characterized as chaotic.

To detect the stability (or non-chaoticity) of orbits about small bodies, the natural **technique** is to use Finite-Time Lyapunov Characteristic Exponents (FTLCE, see [26]). The propagation of uncertainties (covariance) is governed by the state transition matrix associated with a trajectory:

$$P(t) = \Phi(t,t_o)P(t_o)\Phi(t,t_o)^T \tag{29}$$

where $P(t)$ is the state covariance matrix of the S/C at time t and $\Phi(t,t_o)$ is the state transition matrix of the orbit from time t_o to time t. If some eigenvalues of this matrix grow exponentially with time, then the uncertainty along the corresponding eigenvectors will grow exponentially. The FTLCE is a measure of the exponential growth of these eigenvalues:

$$= \frac{\ln \lambda(t)}{t} \tag{30}$$

where χ is defined as the FTLCE, λ is an eigenvalue of the matrix $\Phi(t, t_o)$ and t is the time from the initial epoch t_o. For a true characterization of whether an orbit is chaotic, the FTLCE must be evaluated as time grows arbitrarily large. In practice the computation is considered complete if the FTLCE reaches a finite positive (or negative) value or if it continues decreasing in magnitude as time increases. For practical purposes, we only need to understand the behavior of the eigenvalues over the time the orbit solution is desired to be predictable. Depending on the circumstances, this could range from a few days to weeks or months.

A related issue is the computation of periodic orbits about small bodies (periodic in the body-fixed frame). While these orbits may be of interest on their own right as possible S/C trajectories, they have a deeper significance in terms of the phase space about them. Should a periodic orbit be stable, then trajectories in the surrounding phase space will have regular quasi-periodic motions. This tells the analyst that orbit uncertainties will at most propagate as a polynomial in time, and that the particular S/C orbit will remain bounded and 'safe' for long periods of time.

Conversely, if a periodic orbit is unstable then trajectories in the surrounding phase space will diverge exponentially from the orbit. Furthermore, in this situation, the unstable manifolds of these orbits become important, as they wander over some region of phase space and any S/C orbit which comes sufficiently close to them will fall under their influence, at least temporarily, and follow an exponentially diverging path. Thus, if a set or family of unstable periodic orbits can be found in some region of the phase space, there is a high probability that S/C orbits in this region will be chaotic and will be, inherently, unpredictable to some resolution of measurement. The computation of periodic orbits and their stability is closely related to the computation of FTLCE's. See [18], [19], [21] and [5] for further discussions and computation of periodic orbits about asteroids.

4 Close Proximity Operations

An area of current interest is the navigation and control of a S/C close to the surface of a small body. This is a rather broad concept, however, and several very diverse types of orbits may fit into this general category. In the following sections a few different options for designing close proximity orbits about a small body are given, here assumed to be either an asteroid or an inactive comet.

4.1 Retrograde Orbiters

The simplest, and most inexpensive, manner in which to fly close to the surface of a body is to fly in a retrograde orbit close to the equatorial plane of the body. Such an orbit can be controlled and flown from the ground. This approach assumes that the body is in, or is near, principal axis rotation. In this approach the S/C flies against the rotation rate of the body (i.e. at an inclination of 180°). As was noted previously the orbit will see little variation in its shape or size (even for near-circular orbits). There will be large secular rates in its argument of ascending node and in its argument of periapsis, due to the C_{20} term of the gravity field. Characteristic values of these rates for various bodies are given in [18], [19], [21] in detail. For a circular S/C orbit just above the long ends of a body with a shape ratio of 1:0.5:0.5, these secular rates in these angles are:

$$\dot{\omega} = 6.1\sqrt{\rho}\left(\frac{5}{2}\sin^2 i - 2\right) \text{ degrees/hour} \tag{31}$$

$$\dot{\Omega} = 6.1\sqrt{\rho}\cos i \text{ degrees/hour} \tag{32}$$

$$\dot{M}_o = \tag{33}$$

where ρ is the body density in grams per cubic centimeter. Thus, clearly, an orbit out of the equatorial plane will have substantial precession in inertial space.

Orbits such as these may be extremely stable and useful for safely orbiting an asteroid at low altitudes. In fact, the NEAR mission will fly such an orbit for a sizable fraction of its mission in order to generate high resolution imaging of the surface ([16], [6]). The draw back to such orbits is the high relative **velocities** between the S/C and the asteroid This relative velocity may make it impractical to use these low orbits as s a ing areas for in situ measurements, and can blur high-resolution images of tile surface]'()) our sam model body, the orbital speed in the body-fixed system is approximated as:

$$1 : (0.264\sqrt{\rho} + 1.745/T)\alpha \text{ m/s} \quad (34)$$

where α is the longest dimension of the body in km, T is the rotation period of the body in hours and ρ is the density as before. For a small com I with a slow rotati on and $\rho = 1$ g/cc, $\alpha = 1$ km and $T = 12$ hours, the orbital speed is quite small (~ 0.41 m/s), perhaps making it feasible for some sort of in situ sampling. For an asteroid su ll s Eros, wit h $\rho = 3$, $\alpha = 20$, $T = 5.27$ the relative speed increases to 15.8 m/s, clearly too fast for most conceivable in sit u operations.

The specific orbit which NEAR will fly is a 35 km radius orbit, with relative speeds expected to be on the order of 5- 10 m/s,

4.2 Hovering Orbits: Inertially Fixed

The concept of fixing a S/C's position in inertial space, relative to the small body, is another proposed mode of operation. Reasons for wanting to d tl . vary, the usual being a desire to set up a landing flight or to achieve some in situ measurement not possible from orbit. Another application may be to fix the S/C into an orbit that stays on he sun side of the small body **for** some extended period, perhaps to support an imaging or mapping campaign. Most viable applications **of such** maneuvers are only possible **at very** small bodies.

The **concept of** fixing **a** S/C in inertial space with respect to a sm**all** body is really just an extension of the concept **of a** Lagrangian point about a small body. Indeed, given an appropriately sized and designed thrust control, a S/C can chose an arbitrary point alon g the bod y-sun line to maintain. The necessary thrust to maintain such an orbit is:

$$f \sim \frac{\mu}{r^2} - 3N'^2 r \quad (35)$$

where N' is the small body orbit's angular rate round the sun and r is the S/C distan ce from the small body towards the sun. For the region of interest to us we can ignore the N'^2 term. Then, the cost of maintaining a specified distance from a body using **a** continuously thrusting engine can be computed to be:

$$f \sim 1.0\left(\frac{\rho r_0}{\tilde{r}}\right) \text{ m/sec/hour} \quad (36)$$

where ρ is the body density in g/cc, r_0 i the mean radius of the body and $\tilde{r}$ is the S/C radius non-dimensionalized by the mean radius. Thus the **cost** of hovering at a specified number of radii is proportional to both the density and t he overall size of the body, This approach is clearly feasible for small bodies on the order of a few kilometers. and with the normal range of densities, where hovering may be sustained for a few hours with small ΔV penalty.

Practical implementation of this approach requires autonomous navigation **or accurate** models of the small body and the S/C thrusting system For autonomous control, it is necessary to have a complete estimate of the S/C position, knowledge of the range or altitude alone is not sufficient as the lateral displacement **of** the S/C will be unobserved and could very easily **lead** to the S/C diverging from its desired position Note that, as this class of orbits **are a** generalization **of** the Lagrange points, they also inherit the instability of those orbits. Furthermore, the time scale of their instability is enhanced by the application of additional forces and by moving the S/C closer to the body. An estimate of the time scale of their instability **is** given by:

$$T_s \sim 22.3\sqrt{\tilde{r}/\rho} \text{ minutes} \quad (37)$$

where T_s is the time scale in minutes, $\tilde{r}$ is the radius of the S/C normalized by the mean body radius and ρ is the density of the body in g/cc

Use of such inertially fixed orbits for in situ measurements may not always be applicable. The S/C-body relative speed is not nulled out in this approach, and this can cause significant relative velocities depending on the body rotation rate. Unless sampling occurs at the poles of the body, in situ measurements or sample gathering will probably be better handled by hovering in the body-fixed frame (discussed in the next subsection).

It is not always feasible to use variable thrust engines to achieve the hovering described here. There are some simple schemes that effect the same result, although they are implemented by impulsive maneuvers (i.e. by constant thrust engines). The basic idea is that the S/C is always in an orbit about the body, usually an elliptic orbit with periapsis close to or within the surface. Then the S/C reverses its in orbit velocity, or at least reverses the i component of it, whenever a certain critical radius is passed, in effect forcing the S/C to repeatedly fly through apoapsis. This same idea may be generalized to hyperbolic orbits although in this case the S/C is forced to repeatedly fly through periapsis, which is chosen at a desired altitude. The cost for such operations is always greater than the continuous thrust hovering scheme. For an orbit with eccentricity close to one, the time between maneuvers may be estimated as:

$$T \approx 0.743\sqrt{\frac{(\tilde{r}_a - \tilde{r}_f)\tilde{r}_a^2}{\rho}} \text{ hours} \tag{38}$$

where $\tilde{r}_a$ is the normalized apoapsis of the orbit and $\tilde{r}_f$ is the normalized radius at which the maneuver is triggered. Note that the time between maneuvers is independent of the size of the body. It is also clear, for most situations of interest, that the time between maneuvers will always be on the order of a few hours, which is probably too frequent to reliably control from the ground. Autonomous station-keeping using this approach has been proposed in the past for a phase of operations at a comet.

Navigation data types needed to support such orbits are attitude determination, optical imaging and, in some circumstances, altimetry measurements. If the orbit is maintained far enough from the body, then optical imaging should be sufficient, using measurements of the limbs of the body to determine the relative position of the S/C. Should this approach be used close to the body's surface, then landmark tracking would probably be essential in order to control the lateral motion of the S/C. If hovering very close to the body's surface is desired, then altimetry measurements would be needed to explicitly control the radial rate of the S/C. In this situation, the altitude would be controlled at a higher rate using the altimetry data while the lateral positioning and motion of the S/C could be controlled at a slower rate using the imaging of limbs or landmarks. This fits well with the necessary processing times for each type of measurement, as altimetry has a fast turn around time and optical will in general take longer to process.

4.3 Hovering Orbits: Body-Fixed

For hovering operations close to the surface of a small body it may be more useful to fly in the body-fixed coordinate system. To do this the S/C thrust law should eliminate both the gravitational and the rotational accelerations. Thus the total thrust vector will be of the form:

$$f = 2\Omega \times \dot{\mathbf{r}} + \Omega \times (\Omega \times \mathbf{r}) + \dot{\Omega} \times \mathbf{r} - U_{\mathbf{r}} \tag{39}$$

Since the body-relative speeds and the rotational acceleration of the body will be small this reduces to:

$$f \approx \Omega \times (\Omega \times \mathbf{r}) - U_{\mathbf{r}} \tag{40}$$

which, for purposes of discussion, can be bounded by,

$$f \approx \omega^2 r + \frac{\mu}{r^2} \tag{41}$$

The fuel costs of this approach are similar to the cost of inertial hovering, plus an added term due to the rotational dynamics portion which can be bounded from above by an additional $1\ 1r/T^2$ m/s/hour, where r is in km and T in hours. Proper application of this thrust law will result in a S/C force environment of $\ddot{\mathbf{r}} = 0$ with respect to the central body. Then, assuming that the thrust law can be properly applied the S/C can be flown along pre-programmed rectilinear flight paths about the body. Note that this implicitly assumes that the S/C has a variable thrust engine. Should the engines be fixed thrust, the realization of these orbits becomes much more difficult.

Given reliable position estimates, it is possible to devise a simple closed-loop feedback control system that forces the S/C trajectory to follow the pre-programmed flight path. With such a system implemented, it is no longer necessary to have highly accurate gravity field model. Indeed, simulations where the S/C is given a 4th degree and order gravity field and flown in a full gravity field show that this level of modeling seems sufficient, even when close to the asteroid surface. Such operations seem feasible from a control and fuel point of view at smaller bodies. To show true feasibility, however, will require proving the orbit determination concept and making sure that it is accurate enough to support such flight paths. This is an area of ongoing study.

4.4 "Exotic" Natural Orbits

Once an autonomous navigation system has been developed and applied to the above situations, it can also be applied to other situations. Note that there is a relatively large fuel cost of performing close proximity operations, especially at larger bodies. To reduce these fuel costs and still enable close proximity operations entails the use of natural orbits, or slight deviations from natural orbits, to bring the S/C close to the surface. As discussed in References [18], [19] and [21] there are a wealth of periodic. orbits which come close to the asteroid surface with fairly low relative speeds. Such orbits are, however, unstable and could not be flown from the ground using traditional navigation techniques. To support flight in such an orbit would require an autonomous navigation and control system, conceivably the same system as assumed for the hovering capabilities. Now, the total fuel cost would be that portion necessary to actively control the flight path back to the nominal orbit. Also, it would be possible to control the trajectory to transition along a family of orbits, ending up in an orbit that was close to the surface after starting from a family which was nominally, say, a circular orbit.

This would be, technically, a more challenging feat, but the potential fuel savings could very well make such an approach useful. Of greatest interest would be the interplay between the orbit determination uncertainty and the control law implemented by the S/C, as this could potentially be an unstable system. This would be due to the non-linear interaction between the orbit uncertainty and the chaotic mapping of these orbits into the future.

The technical scheme to follow would be to precompute the desired periodic orbit and the necessary transfer orbits on the ground and load this up onto the S/C as it's nominal flight plan. Depending on the specific orbit, the ground team may also want to precompute the control and orbit determination strategy, in terms of amount and timing of measurements and placement of control maneuvers.

5 Landing Orbits

Landing and orbital operations at asteroids can be categorized with respect to their strategy and intent. Three major categories can be drawn: soft landing, hard landing and high-speed impact. A soft landing is characterized as a controlled descent where the intent is to minimize the impact speed of the spacecraft. Usually implicit in this approach is the ability to accurately steer towards specific landing sites. A hard landing is a landing sequence initiated from orbit which does nothing to control (i.e. minimize) the impact speed of the spacecraft. In both of these landing scenarios it is necessary for the spacecraft to rendezvous and orbit the asteroid prior to the landing sequence. If an accurate physical model of the target, e.g. from radar images, is not available the orbital phase may last until the shape, rotational dynamics, and gravity field of the asteroid is determined. For a high-speed impact with a body the spacecraft does not enter orbit about the asteroid but proceeds directly from hyperbolic approach to impact.

5.1 High Speed Impact

The intent is to impact the asteroid with a high speed (on the order of several hundred to several thousand meters per second) to observe the ejecta field from that impact from a mother or sister S/C. The impact speed may be controlled by performing a maneuver some days before impact to adjust the impact speed and to re-target the spacecraft toward the center of the asteroid. Following this maneuver, a final correction and retargeting maneuver will have to be made shortly before impact using optical data taken during the approach. If the asteroid has been observed with radar prior to impact the optical data may not be necessary, so long as the spacecraft impact uncertainty ellipse is much smaller than the body. Even if the body's ephemeris is perfectly known, if the inertial orbit determination of the spacecraft is poor optical sightings will still be necessary.

Given optical images of the body against the star background, the uncertainty of the spacecraft trajectory in the impact plane can be approximated as $\sigma_d \sim R\sigma_\alpha = V_I T \sigma_\alpha$, where σ_d is the uncertainty radius in the impact plane, R is the spacecraft range to the body at the time of observation, σ_α is the angular accuracy with which the body may be located, V_I is the impact speed, and T is the time to impact. The angular accuracy is a combination of the camera pixel size (or suitable fraction thereof) and the ability of the optical data processor to model the shape of the target body (i.e. estimate the center-finding error):

$$\sigma_\alpha = \sqrt{\sigma_p^2 + (f_d d/R)^2} \tag{42}$$

where σ_p is the pixel size of the camera, f_d is a fraction describing the ability of the measurement processor to characterize or estimate the center of the body (usually < 0.25 at least), d is the mean diameter of the body and R is the S/C range from the body at the imaging time. Then the data cutoff time to achieve a specified accuracy is

$$T = \frac{d}{V_I \sigma_p}\sqrt{(\sigma_d/d)^2 - f_d^2} \tag{43}$$

Clearly, an important limiting factor for the ability of the S/C to target an impact trajectory involves the ability of the measurement processor to estimate the target center once it becomes resolved. For a specific example assume an impact speed of 1 km/s, a desired uncertainty in the impact plane of 0.27 diameters, and a center-finding error fraction of 0.25, then $T \sim 0.1\, d/\sigma_\alpha$ (seconds). Typical camera accuracies may range from 0.1 mrad (for an inaccurate camera) to 1 μrad for an accurate camera, providing data cut-off" times which range from 17 minutes to 1.2 days, respectively, for a 1 km body.

The size of the final maneuver is a function of the previous control errors and the relative ephemeris uncertainty of the target body. The necessary maneuver size is just the error divided by the time to impact. Assuming an incoming targeting error of 10 km, this translates into a 10 m/s burn for the inaccurate camera and a 0.1 m/s burn for the accurate camera, again for a 1 km body. Clearly, there is a fuel cost associated with a less accurate camera for this approach.

In general, such a craft will be considered "expendable" and will probably not have high accuracy imaging devices on board but will have a low accuracy optical device instead. Then, with the shorter time spans associated with an inaccurate camera, an autonomous navigation system will probably have to be incorporated to support the final targeting maneuver. The sophistication of this system is not great, as all it must do is find the target center in the images and design maneuvers to move the target center to the S/C boresight.

5.2 Hard Landing

A hard landing can be defined as a ball stic drop from orbit onto the asteroid surface with no braking maneuver prior to impact. This approach is attractive as it involves no thrusting maneuvers to control the descent rate and avoids some of the small body modeling issues by passing relatively swiftly to the asteroid surface. The achievable landing accuracy on the asteroid surface will be a function of the orbit determination accuracy, maneuver execution errors and asteroid modeling errors. The orbit from which the lander is delivered will also play a role in the landing accuracy and impact speed.

The impact speed of such a lander is approximated by a few simple formulae. First, assume that the spacecraft velocity with respect to the asteroid is nulled out at some normalized radius $\tilde{r}_a$ and the spacecraft is allowed to fall onto an asteroid of radius r_o. Then the impact speed is, approximately:

$$V_I \approx 0.75\sqrt{\mu r_o}\sqrt{1 - \frac{1}{\tilde{r}_a}} \text{ m/s} \tag{44}$$

For control purposes a non-zero speed may be imparted to the spacecraft at the de-orbit maneuver (this will provide angle of attack control at impact). The corresponding impact speed is computed by taking the root-sum-square of that speed with Equation 44.

For a maneuver performed at periapse the control error in the impact site can be approximated as:

$$\sigma_b \approx \sqrt{(f_r r_p \sqrt{1+e})^2 + \sigma_r^2} \tag{45}$$

where σ_b is the error in the impact plane, f_r is the fractional error in the executed maneuver (typical values range from 0.001 to 0.02), r_p is the delivery orbit periapsis, e is the delivery orbit eccentricity and σ_r is the position uncertainty at the time of the maneuver (the delivery orbit is the orbit prior to the de-orbit maneuver). A more thorough analysis of delivery accuracy to the surface of a comet for a specific case is addressed in [23].

5.3 Soft Landing

A soft landing can be realized in a number of ways, the two of greatest interest depend on the type of thrusters used by the S/C; whether the engines have a fixed or variable thrust level. In the following subsections we sketch out the fundamentals of the dynamics for each approach.

5.3.1 Fixed Thrust Level

This approach is appealing as most S/C thrusters are designed to impart a fixed level of thrust and cannot be easily modulated in real time to deliver variable levels of thrust. Also, this approach is more amenable to pre-programming from the ground and thus may eliminate the need for autonomous navigation for support.

The basic scenario is as follows: the S/C de-orbits at some radius r_b and begins a free-fall towards the body ($V_b = 0$). At a radius r_I the constant thrust engine is activated burning in a fixed direction (i.e. towards the body) with an effective acceleration of f (assumed to be constant over the time interval of interest). If the above parameters are properly chosen, then the S/C will impact the body surface with a speed V_I. The problem to solve is, given a de-orbit radius r_b, a S/C acceleration f, a given body and a desired impact speed V_I, at what altitude r_a should the thrusters be ignited.

During the thrusting portion of the fall, assume that the S/C is moving entirely in the radial direction, then the equations of motion become

$$\ddot{r} = -\frac{\mu}{r^2} + f \tag{46}$$

This equation has an integral, found by multiplying through by $\dot{r}$ and integrating:

$$\frac{1}{2}V^2 = \frac{\mu}{r} + fr - \left(\frac{\mu}{r_a} + fr_a - \frac{1}{2}V_a^2\right) \tag{47}$$

This equation can relate the impact speed (when $r = r_o$) with the S/C radius and speed at thruster ignition. Now, note that the burn ignition will occur at a different radius than the initial de-orbit burn, and that these two states are related by the Keplerian energy to arrive at:

$$\frac{1}{2}V^2 = \frac{\mu}{r} + fr - \left(\frac{\mu}{r_b} + fr_a\right) \tag{48}$$

This relationship can be used to relate the various parameters of this problem. If burn termination is scheduled to occur at radius r, before impact at radius r_o, then the impact speed becomes:

$$\frac{1}{2}V_I^2 = \frac{1}{2}V^2 + \frac{\mu}{r_o} - \frac{\mu}{r} \tag{49}$$

Note that the acceleration is constrained such that

$$f \leq \frac{\mu}{r_a - r}\left(\frac{1}{r} - \frac{1}{r_b}\right) \tag{50}$$

This ensures that the S/C speed does not pass through zero, which would imply that the S/C would begin to escape from the body.

For simplicity, assume that the burn termination occurs at landing ($r = r_o$) and that the impact speed is specified ($V = V_I$), then the radius at which the burn must be ignited is:

$$\tilde{r}_a = 1 + 0.279\frac{\rho r_o}{f}(1 - 1/\tilde{r}_b) - \frac{V_I^2}{2fr_o} \tag{51}$$

where $\tilde{r}_a$ and $\tilde{r}_b$ are the normalized radii where burn ignition and the de-orbit maneuver occur, ρ is density in g/cc, r_o is body radius in km, f is S/C acceleration in mm/s^2 and V_I is impact speed in m/s.

Now let us briefly consider an example. Given a 500 kg S/C with a total thrust of 4 N, the acceleration f = 8 mm/sec. Assume the body is an asteroid with radius 10 km and density 3 g/cc. Finally, assume that the de-orbit maneuver occurs at 5 asteroid radii (50 km) and assume landing speeds of 1, 0.5 and 0.1 m/sec. The respective altitudes at which burn ignition must be made are then: 18,307, 18.354, 18.369 km. The limiting altitude before the S/C will escape prior to impact is 18.370 km. It is clear that the impact speed is sensitive to the ability of the S/C to ignite the thrusters at the proper radius and that for a very slow impact speed (say 0.1 m/s) an error of 1 meter can cause an escape.

Given these sensitivities, it would be useful to incorporate altimeter measurements during the descent phase. Otherwise the burns would be initiated by an internal clock, with burn time based on the pre-deorbit maneuver orbit determination, and is likely to be in error. For this example, the approximate speed at burn ignition is about 76 m/sec. If no other measurements are made, the radius determinations will be limited by the propagation errors of the S/C and the modeling errors of the body. If the propagation errors prove to be too large, they can be reduced by adding landmark or limb tracking to the on-board navigation, down to reduce the error to the body modeling error.

Not considered above are the nonspherical effects of the body and the rotational dynamics of the body. Given a specific, desired impact state and a body model, the appropriate burn ignition times or radii could be computed on the ground and loaded into the S/C program. This approach should work well for larger impact speeds and could be implemented by the NEAR S/C at the end of its nominal mission phase, should it be desired to land that S/C onto the Eros surface.

5.3.2 Variable Thrust Level

The alternative approach would be to supply the S/C with a variable thrust system. The particulars of building such a thruster system are not discussed here but many possible approaches should exist, from modulation of the mass-flow rate to implementation of a pulsing strategy. While this approach is not necessary for landing on a small body, it would enable greater freedom in controlling the descent phase and actually picking or steering towards a particular landing site on the surface of the asteroid.

To use such a capability' toits fullest potential would require an autonomous orbit determination and control algorithm on board the S/C. The body-relative position determination would be used to compute the thrust to null the gravity field, which would be represented as a truncated spherical harmonic field with the appropriate rotational dynamics model. The S/C would also be given a nominal flight, path in the body-fixed frame which could include periods of hovering, lateral motion and vertical motion. The scenario would be very similar to that discussed in the previous section on hovering orbits in the body-fixed frame. The S/C trajectory would be controlled by a closed loop feedback control which would process position measurements to determine a state estimate and a state error, which would be the difference between the estimate and the desired state at a given time. Suitable gain constants would be applied to these errors to drive the S/C back to its nominal trajectory.

Simulations applied to a realistic shape model of the asteroid Toutatis establish the feasibility of the closed loop control. Yet to be evaluated is the stability of this scheme in the presence of larger orbit determination errors, that analysis is currently being performed.

The necessary thrust will be bounded by :

$$f \lesssim [\rho/r^2 \ [illegible] \ (1.9 \cos\delta/T^2] \text{ m/s/hour} \quad (52)$$

$$\sim 28[\rho/r^2 \ [illegible] \ \cos\delta/T^2] \text{ micro g's} \quad (.53)$$

where T is the body's rotational period in hours, and δ is the S/C latitude as measured from the rotational equator. Note that implementation of this thrust law without feedback control will be unstable. If the precise location on the surface is not of interest, the loop can be closed with altimetry measurements, so long as the lateral drift of the S/C can be bounded using open-loop control. If lateral motion cannot be bounded, or landing is desired at a precise location on the surface, then landmark tracking should be used in conjunction with altimetry data.

The above formulae are useful only for order of magnitude design purposes. When considering an actual trajectory the role of the irregular shape and gravity field of the asteroid becomes very important, both from the standpoint of spacecraft dynamics and from the standpoint of reducing any measurements taken during descent. Improper modeling of either of these may lead to an incorrect maneuver or thrust level and a consequent escape or "harder" landing on the asteroid surface.

5.4 Surface Operations and Return to Orbit

Once on the surface, if the spacecraft is to remain it will be important to have an accurate model of the surface gravity field, which will be weak and possibly irregular. A sensible strategy is to use a polyhedron model, which provides the exact constant density gravitational field for an arbitrary polyhedron ([24]). This field is non-singular at the surface of the body and can be easily modified to account for local density inhomogeneities.

Given a successful soft landing on an asteroid, the design and implementation of a return trajectory is much simpler. A typical sequence would consist of at least three pre-programmed burns: an initial burn to lift the spacecraft from the asteroid surface to some altitude, followed by a burn to turn that altitude into the orbit periapsis and move the orbit apoapsis a safe distance from the surface, followed by a third burn at orbit apoapsis which raises periapsis to a high, safe altitude.

6 Conclusions

Given in this paper was a discussion ,111 theop ratio and dynamics of a S/C close to a small body, such as an asteroid or comet. The main purpose of this paper was to bring realism **to** some **of the** discussions which are occurring concerning s c missions, discussions which sometimes arc vastly oversimplified or which ignore some crucial element or realities that must be dealt with early-on in the design phase for such missions.

The results are not meant to be all inclusive although a stress has been lain on keeping the results general enough to be useful to a wide range of different body shapes and sizes. To that end, a number of order-of-*magnitude* design formulas have been derived and stated, concentrating on those dynamical aspects likely to be of greatest interest to the mission designer such as landing speed and fuel cost.

A truly exciting possibility will occur during and after the main operations phase of the NEAR mission to the asteroid Eros. During the phase the S/C will come within ~ 3 mean radii of the body for extended period.s of time, subjecting the S/C orbit **10** large perturbations **and** serving **as a check 011 our** understanding **of** this orbital environment. Then, following the end of the prime mission, a possibility exists that the S/C will be allowed to land on the asteroid surface, thus serving as the fore-rullrlcr of, what is to be hoped to be future such craft to other small bodies in our solar system

Acknowledgments

The research described in this paper was carried out by the Jet Propulsion Laboratory, California Institute of Technology, under contract with the National Aeronautics and Space Administration.

References

[1] S. Bhaskaran, J.E. Riedel & S.P. Synnott "Demonstration of Autonomous Orbit Determination Around Small Bodies", AAS/AIAA Astrodynamics Conference, Halifax, Nova Scotia, Aug 1995

[2] D. Brouwer, "Solution of the Problem of Artificial Satellite Theory Without Drag", The Astronomical Journal, 64, 378 - 397, 1959

[3] B. Chauvineau, P. Farinella & t Mignard "Planar Orbits about a Triaxial Body: Application to Asteroidal Satellites", Icarus 105, 37) 38 1993

[4] J.M. A. Danby, Fundamentals of Celestial Mechanics, 2nd Ed., Willmann-Bell, 1988.

[5] E. de Jong, S. Suzuki 1995. "Visualization of Earth Approaching Asteroids and Associated Physics using Radar Based Models", AVC-95-147, Catalog on-line at: http://www.jpl.nasa.gov/archive/vidcat.html

[6] R. Farquhar, D. Dunham, J. McAdams, "Mission Overview and Trajectory Design", J. Astronautical Sciences, Vol 43, No 4, 1995 in Press

[7] B. Garfinkel, "On the Motion of a Satellite of an Oblate Planet", The Astronomical Journal, 63, 88-96, 1958

[8] R.W. Gaskell, "Digital Identification of Cartographic Control Points", Photographic Engineering and Remote Sensing, Vol 54, No 6, Part 1 June 1988

[9] R.S. Hudson, S.J. Ostro, "Shape and Non-Principal Axis Spin Slate of Asteroid 4179 Toutatis", *Science*, 270, 1995, 84-86.

[10] R.S. Hudson, S.J. Ostro, "Shape of Asteroid 4769 Castalia (1989 PB) from Inversion of Radar Images", *Science*, 263, 1994, 940 943.

[11] R.S. Hudson, "Three-Dimensional Reconstruction of Asteroids from adar Observation", *Remote Sensing Rev.*, **8**, 1993, 195 - 20.

[12] W.M. Kaula, Theory of Satellite Geodesy, Blaisdell, 1966

[13] Y. Kozai, "The Motion of a Close Earth Satellite", The Astronomica Journal, 64, 367-377, 1959

[14] W.D. MacMillan, Dynamics of Rigid Bodies, Dover 1960

[15] S. Mottola, et al., "The slow rotation of 25 Mathilde", Planetary and Space Science, 1995, in press

[16] J.K. Miller, W.E. Bollman, R.P. Davis, C.E. Helfrich, D. J. Scheeres, S,1'. Synnott, T.C. Wang, B. Williams, D.K. Yeomans, "Navigation Analysis for Eros Rendezvous and Orbital Phases", J. Astronautical Sciences, Vol 13. No 1.199, in press

[17] S. J. Ostro, "Radar Observations of Near Earth Asteroids", in *Spaceflight Mechanics 1995*, Advances in the Astronautical Sciences Series, Vol. 89. Univelt, San Diego, California 1994.

[18] D. J. Scheeres, S.J. Ostro, R. S. Hudson, R A Werner, "Orbits Close to Asteroid 4769 Castalia", Icarus, **121**, pp 67-87, 1996

[19] D. J. Scheeres, "Analysis of Orbital Motion Around 433 Eros", Journal of the Astronautical Sciences, Vol 43, No 4, 1995 (in press

[20] D.J. Scheeres, B. G. Williams, W '.} Bollman R.P Davis, C.E. Helfrich, S.P. Synnott, D. K. Yeomans, "Navigation for Low-Cost Missions to Small Solar System Bodies", Acta Astronautica, Vol 35, Suppl., pp 211 - 220, 1995

[21] D. J. Scheeres, "Dynamics about Uniformly Rotating Tri Axial Ellipsoids: Applications to Asteroids", Icarus **110**, 225- 238, 1994

[22] D.J. Scheeres, "Satellite Dynamics About Asteroids", in Spaceflight Mechanics 1994, Advances in the Astronautical Sciences Series, Vol 87 No. 1, 1994, pp 275 292.

[23] R. M. Vaughan, "Navigation Covariance Analysis for Rosetta SS}' Descent", JPL IOM 314.3-1128, September 23, 1994, *internal document*

[24] R.A. Werner, "The Gravitational Potential of a Homogeneous Polyhedron", *Celestial Mechanics*, **59**, 1994, 253-278.

[25] R. A. Werner & D.J. Scheeres, "Polyhedron Gravitation", in review, 1996.

[26] S. Wiggins, Non-linear Dynamics, Springer- Verlag, 1992

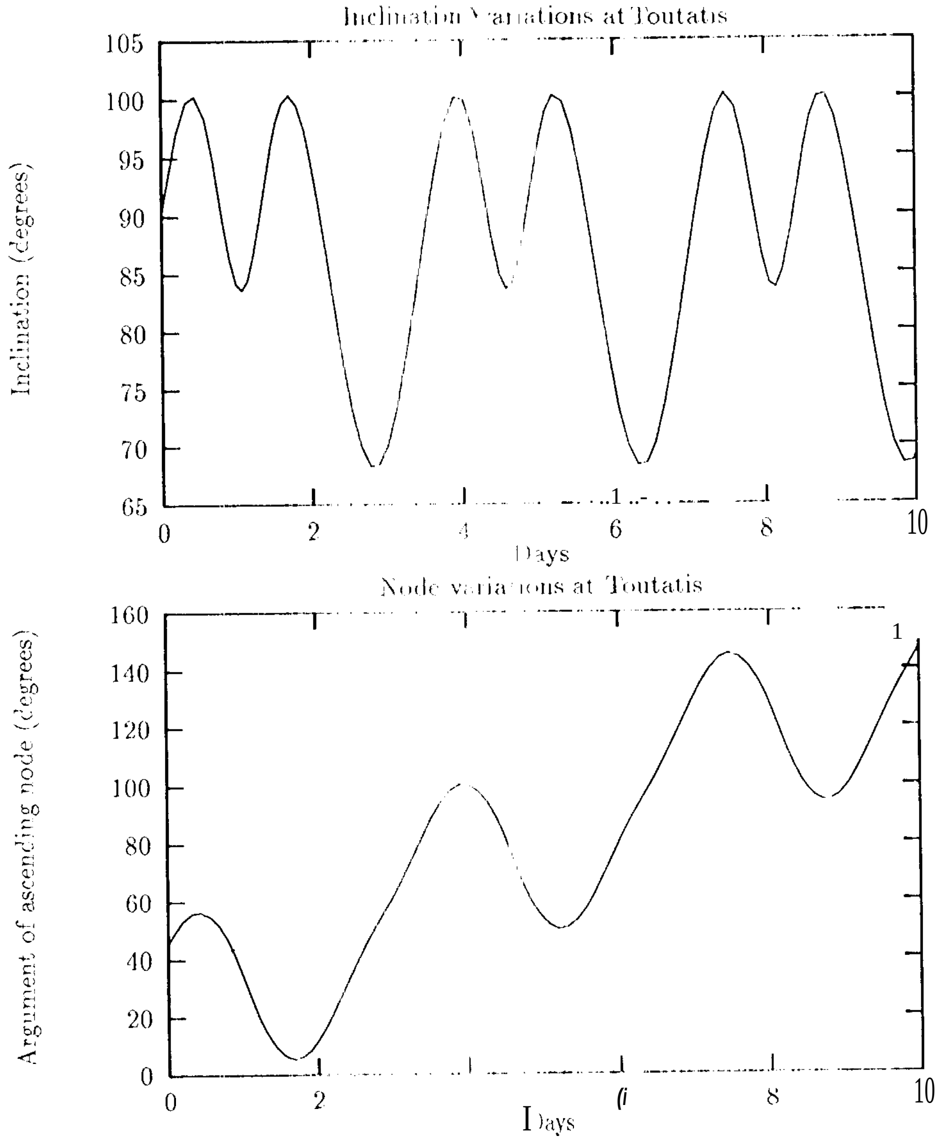

Figure 2: Inclination and node variations over 10 days for a circular Toutatis orbit in a ~ 2.5 mean radii orbit.

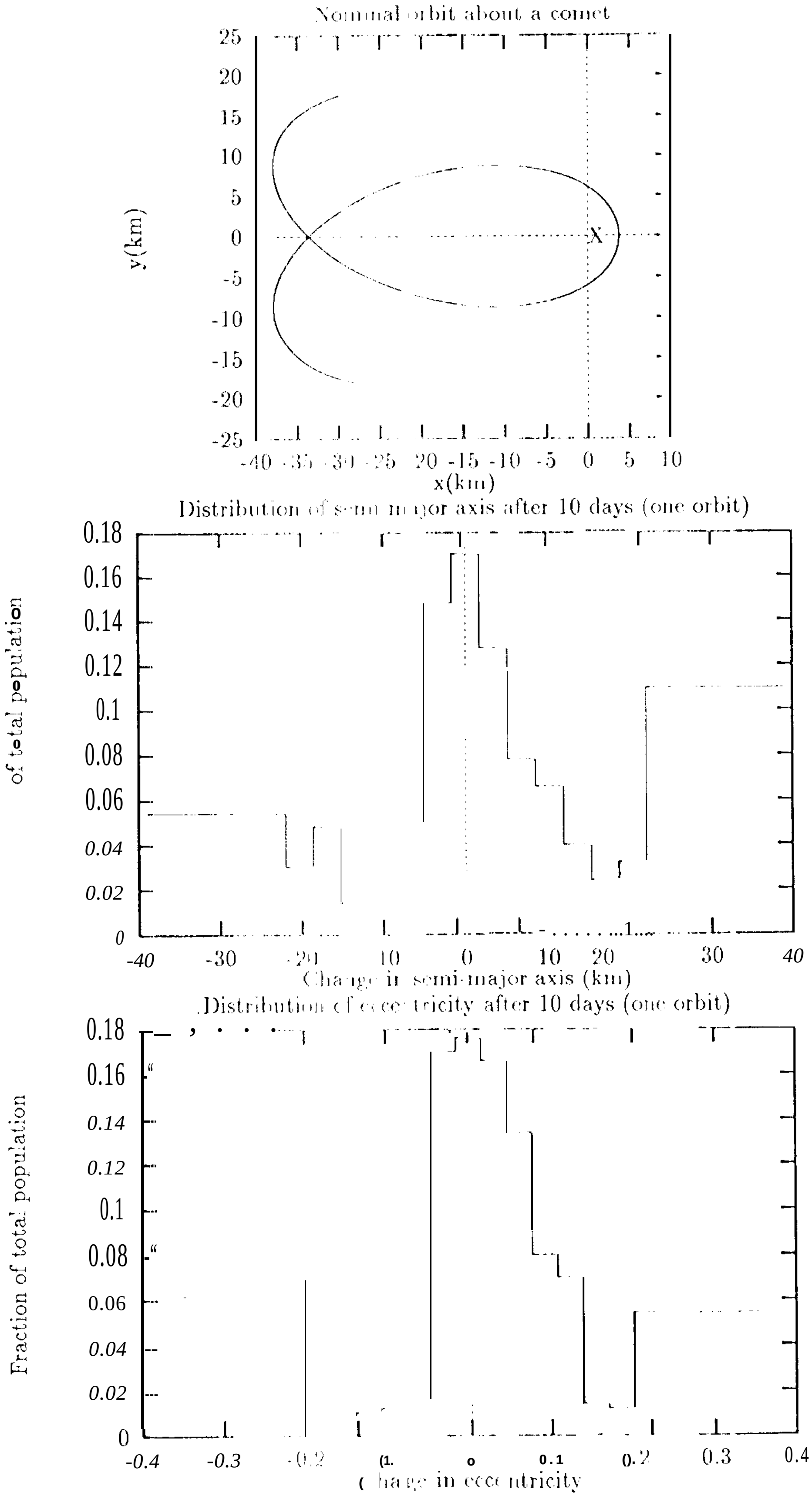

Figure 3: Nominal orbit and histograms of change in semi major axis and eccentricity after 10 days with an initial position and velocity uncertainty of 5 meters and 0.1 mm/sec, respectively